J. Fluid Mech. (1999), *vol.* 398, *pp.* 61–85. Printed in the United Kingdom

Nonlinear stability of mixed convection flow under non-Boussinesq conditions. Part 1. Analysis and bifurcations

By S. A. SUSLOV† AND S. PAOLUCCI

Department of Aerospace and Mechanical Engineering, University of Notre Dame, Notre Dame, IN 46556, USA

(Received 10 January 1998 and in revised form 26 May 1999)

The weakly nonlinear theory for modelling flows away from the bifurcation point developed by the authors in their previous work (Suslov & Paolucci 1997) is generalized for flows of variable-density fluids in open systems. It is shown that special treatment of the continuity equation is necessary to perform the analysis of such flows and to account for the potential total fluid mass variation in the domain. The stability analysis of non-Boussinesq mixed convection flow of air in a vertical channel is then performed for a wide range of temperature differences between the walls, and Grashof and Reynolds numbers. A cubic Landau equation, which governs the evolution of a disturbance amplitude, is derived and used to identify regions of subcritical and supercritical bifurcations to periodic flows. Equilibrium disturbance amplitudes are computed for regions of supercritical bifurcations.

1. Introduction

The mixed convection flows considered in this paper typically exist in such technical applications as chemical vapour deposition reactors, heat exchangers, thermal insulation systems and others. In many of these applications, the characteristic temperature difference is comparable with the average temperature of the fluid and the temperature gradients are sufficiently large to cause essential fluid property variations (Chenoweth & Paolucci 1985, 1986; Suslov & Paolucci 1995*b*) which cannot be neglected. Quantitative predictions of flow characteristics such as heat transfer rate or mass flux through these systems is a non-trivial task (Suslov & Paolucci 1995*a*, *b*, 1997). Indeed, when the properties of a fluid are allowed to vary with temperature and pressure, the momentum and energy equations, which are used to describe the flow of the fluid, become substantially more complicated due to additional nonlinearities arising from density, viscosity, thermal conductivity and specific heat variations. The property variations lead to the appearance of additional governing parameters in the problem. Thus the cost of direct numerical simulations of such flows for all regimes of interest is prohibitively increased. For this reason we have undertaken to study the character of such flows as a function of the important dimensionless parameters using weakly nonlinear analysis.

In our earlier works (Suslov & Paolucci 1995*a*, *b*) we successfully used the low-Mach-number approximation of the Navier–Stokes equations, instead of the Boussi-

† Current Address: Department of Mathematics and Computing, University of Southern Queensland, Toowoomba, Queensland 4350, Australia.

nesq model, to account for the fluid properties variations and analyse the linear stability of the conduction state in a vertical cavity and open channel. It was shown that the stability characteristics such as the critical Grashof number and the disturbance wave speed depend strongly on the temperature difference when fluid properties are allowed to vary. Moreover, the large density variations, caused by a large temperature difference between the walls, can lead to the appearance of a new buoyant instability which competes with the shear-driven one predicted by the linear analysis of Boussinesq flows.

Linear theory is a universal and powerful technique used to find the location of bifurcations in parameter space, as well as to predict the form of developing disturbances. Unfortunately, one cannot obtain the amplitudes of such disturbances using linear theory and, consequently, provide any quantitative information about a disturbed flow. Thus, it is necessary to consider nonlinearities in order to close the problem. Weakly nonlinear theories developed to date (Stuart 1960; Watson 1960; Stewartson & Stuart 1971), and their modifications (Reynolds & Potter 1967; Sen & Venkateswarlu 1983), have been shown to be very powerful tools for the analysis of stability of various flows. The term 'weakly' is used in the application of nonlinear theories to emphasize that such theories use certain expansion procedures and require the presence of some 'small parameter', the powers of which are used to construct recursively systems of relatively simple (linear) equations whose solutions constitute the terms of asymptotic series. These time-dependent series, if convergent, represent developing disturbances superposed on the primary flow. The choice of a small expansion parameter varies from one approach to another: linear amplification rate, relative distance from the marginal stability surface in the governing parameter space, and the disturbance amplitude itself. Although in the vicinity of a bifurcation point all these approaches lead to similar results, the ranges of convergence of the asymptotic series (and of validity of the analysis) depend strongly on the choice of the expansion (Yao & Rogers 1992). Moreover, the relative distance from the neutral stability curve cannot be used as a small parameter when linear analysis shows that the basic flow is always stable and no neutral surface exists, such as in plane Couette or pipe Poiseuille flows. The same restriction applies when the linear amplification rate is assumed small, since this would be so only close to the marginal stability surface. The most natural and general approach seems to be when expansions are made based on a small disturbance amplitude assumption. Since disturbance amplitudes can possibly remain small for relatively large distances from the bifurcation point, such a technique could potentially remain valid for larger parameter ranges and it can be applied even to flows for which marginal surfaces do not exist (Davey & Nguyen 1971). The validity of the small-amplitude assumption has to be checked *a posteriori* when nonlinear equilibrium states are formally computed. The application of an amplitude expansion (Watson 1960) is typically done in conjunction with a multiple-timescale technique where the fast timescale corresponds to the exponential disturbance time development as predicted by linear analysis. Slower timescales correspond to stages when the growth or decay of the disturbances is influenced by nonlinearities of different orders. Frequently, it is argued that the introduction of multiple timescales is reasonable only when linear disturbances change slowly with time, i.e. when their linear amplification or decay rates are small, since in this case the linear development stage is sufficiently long. We should note here that the length of the linear stage is not a factor defining the validity of the introduction of multiple timescales. The multiple-timescale approach is valid no matter how large the linear amplification rate is, provided that the amplitude dynamics changes substantially as the disturbance

develops. This is always the case if an equilibrium state exists. Then the fast timescale corresponds to the amplitude dynamics away from saturation, while slow scales are introduced for nearly equilibrium regimes.

After amplitude and multiple-timescale expansions are made, separation of different orders in amplitude leads to successive sets of linear equations. An integral solvability condition must be satisfied in order to find a solution close to the marginal stability surface (Stewartson & Stuart 1971; Stuart 1960; Watson 1960). This approach is used to find the value of the constant entering the Landau equation which describes the time-dependent behaviour of the disturbance amplitude. The value of the Landau constant typically is found using appropriate integrals of the eigenfunctions computed at the critical point. This automatically limits the applicability of nonlinear theories to a close vicinity of the bifurcation point. On other hand the eigenfunctions of the linearized problem and their integrals can be computed at an arbitrary point in parameter space regardless of the actual location of the criticality. This suggests using them to determine the Landau constant for an arbitrary set of governing parameters. Unfortunately, this approach faces an inherent difficulty. As was first noted by Herbert (1983), the equations at third order in amplitude become unconditionally solvable when the linear amplification rate is not equal to zero. Thus the application of a solvability condition for the evaluation of the Landau constant becomes meaningless. In order to avoid this difficulty in determining the Landau constant, Herbert proposed fixing the disturbance at some particular spatial point such that it is determined completely by the eigenfunction of the linear problem. We have shown in Suslov & Paolucci (1997) that this procedure leads to an inconsistency in the definition of the equilibrium disturbance amplitude and, subsequently, we have proposed replacing the solvability condition with an appropriate orthogonality condition when analysing supercritical or subcritical flows. The idea of orthogonalizing the solutions of successive systems of equations resulting from weakly nonlinear analysis can be found in Sen & Venkateswarlu (1983), but in Suslov & Paolucci (1997) it was shown rigorously that it is not only desirable, but also necessary. Thus the theory we developed in Suslov & Paolucci (1997) does not require amplitude expansions to be based on the eigenfunctions of the linearized problem computed at the critical point, but rather at a particular point of interest in the parameter space. Consequently, a typical limitation of weakly nonlinear theories to the relatively small neighbourhood of the bifurcation point is relaxed such that, presumably, our approach remains valid for larger distances from criticality.

There are two major differences between Boussinesq and non-Boussinesq flows in the light of the weakly nonlinear analysis. First, in the Boussinesq limit, where fluid properties are assumed to be constant, the governing equations have a quadratic nonlinearity. However, in non-Boussinesq regimes the nonlinear character of the equations is largely governed by the form of the constitutive equations for the fluid, and in general it is not even of polynomial character. This is the case, for example, when the well-known Sutherland formulae are used to describe viscosity and thermal conductivity variations with temperature. Recently, the present authors extended the application of Watson's (1960) theory to the stability of the flow of a general fluid (Suslov & Paolucci 1997). The form of the expansion was rigorously derived based on Taylor expansions of properties about the reference distributions. This enabled us to examine successfully the stability of non-Boussinesq natural convection in a vertical cavity subjected to large temperature differences (Suslov & Paolucci 1997) and to predict mean flow characteristics and disturbance amplitudes at substantial distances from the critical points.

Second, in contrast to the Boussinesq case, under non-Boussinesq conditions the density of the fluid can change with time. This means that in general the total mass of the fluid in an open system changes. Such a situation requires a special treatment in the weakly nonlinear analysis, which to the authors' knowledge has not been discussed properly in the literature to date. In the present paper an important modification of the continuity equation valid for low-Mach-number flows is proposed in order to extend our previously derived theory to flows in open geometries. In this case the total mass of the fluid can vary because of disturbance development. This total mass change affects the mean flow of the fluid and, consequently, the average characteristics of the flow which are of primary interest to engineers.

The amplitude expansion method has been used successfully for supercritical flows. Severe difficulties arise though in applying it in subcritical regimes where the linear amplification rate is negative. Mathematically it becomes impossible to solve the system of linear equations at certain points in wavenumber space. These points correspond to so-called mean flow resonances. Physically this means that there is a strong interaction between the mean flow variation induced by the finite-amplitude periodic disturbance and the time-dependent mean flow itself. The more subcritical the flow is, the more resonance points exist (Davey & Nguyen 1971). Reynolds & Potter (1967), to get around this difficulty, proposed considering the 'false problem' for subcritical flows where the time evolution of disturbances is neglected and only steady equilibrium amplitudes are sought (assuming they exist). Mathematically this approach does not lead to any difficulties when, for example, threshold amplitudes for the subcritical plane Poiseuille flow are estimated. On other hand, the values predicted are in poor agreement with experimental results (e.g. by Nishioka, Iida & Ichikawa 1975). One of the reasons for the disagreement could be that this proposed mathematically simple approach does not account for important physical mechanisms which are present in real flows. Thus, in the present work, the authors prefer to use the 'true problem' approach where complete amplitude dynamics is considered. However, in treating subcritical regimes, we stay away from the resonant points where the present single mode analysis is not adequate. We note that the effects of resonances could be analysed by using a system of the coupled Landau equations, but this is beyond the scope of the present work.

Finally, we note that in Suslov & Paolucci (1995*b*) we carried out a linear stability analysis of non-Boussinesq mixed convection flow in a vertical channel and determined the bifurcation points, where transitions from parallel shear flows to periodic flows occur, for a complete range of governing parameters. A number of physically distinct instabilities not found in Boussinesq flows, as well as codimension-2 points, where instability modes compete with each other, were identified. In the first part of the present paper we augment the previous findings with the analysis of bifurcations and quantitative estimations of equilibrium disturbance amplitudes in post-bifurcation states while in the second part (Suslov & Paolucci 1999) we discuss mean flow distributions and energetics corresponding to different modes of instability.

This part of the paper is organized as follows. First, the problem is formulated for two physically distinct cases: fixed average longitudinal pressure gradient and fixed average mass flux through the channel. Next, the expansion procedure is outlined and properties of the resulting system of equations are discussed. Special attention is paid to the treatment of the mean flow in a system with variable total mass. Finally, the theory is applied to the non-Boussinesq mixed convection flow of air in a vertical channel. Results are given for a wide range of Grashof and Reynolds numbers, and temperature differences between the walls.

2. Problem definition and governing equations

We consider a two-dimensional mixed convection flow between two vertical infinite plates separated by a distance H. We limit ourselves to two-dimensional flows since linear stability analysis (Suslov & Paolucci 1995*b*) shows that the mixed convection flow becomes first unstable with respect to two-dimensional disturbances. The plates are isothermal and maintained at the different temperatures T_h^* and T_c^* ($<T_h^*$) respectively (asterisks denote dimensional quantities). The channel is placed into a uniform vertical gravitational field $\boldsymbol{g}$. Since we are interested primarily in the case of large temperature differences $\Delta T = T_h^* - T_c^*$, the conventional Boussinesq approximation is not applicable and we adopt the low-Mach-number approximation (Paolucci 1982) for the Navier–Stokes equations in order to describe such a flow:

$$\frac{\partial}{\partial t}(\rho u_i) + \frac{\partial}{\partial x_j}(\rho u_i u_j) = -\frac{\partial \Pi}{\partial x_i} + \frac{Gr}{2\epsilon}(\rho - 1)n_i + \frac{\partial \tau_{ij}}{\partial x_j}, \tag{1}$$

$$\rho c_p \left(\frac{\partial T}{\partial t} + u_j \frac{\partial T}{\partial x_j}\right) = \frac{1}{Pr}\frac{\partial}{\partial x_j}\left(k\frac{\partial T}{\partial x_j}\right), \tag{2}$$

$$\frac{\partial \rho}{\partial t} + \frac{\partial \rho u_j}{\partial x_j} = 0, \tag{3}$$

where

$$\tau_{ij} = \mu\left[\left(\frac{\partial u_i}{\partial x_j} + \frac{\partial u_j}{\partial x_i}\right) - \frac{2}{3}\delta_{ij}\frac{\partial u_k}{\partial x_k}\right]. \tag{4}$$

Here $u_i = (u, v)$ and $x_i = (x, y)$ are velocity components and coordinates in the horizontal and vertical directions respectively, and $n_i = (0, -1)$ is a unit vector in the direction of gravity. The boundary conditions for the problem are

$$u = v = 0 \quad \text{and} \quad T = 1 \pm \epsilon \quad \text{at} \quad x = 0, 1. \tag{5}$$

The above system is complemented by the equation of state and property variations

$$\rho = \rho(T), \quad c_p = c_p(T), \quad \mu = \mu(T), \quad k = k(T), \tag{6}$$

where ρ is the fluid density, μ is the dynamic viscosity, k is the thermal conductivity, and c_p is the specific heat at constant pressure, all dependent on the local temperature T. The equations are non-dimensionalized by the use of channel width H, reference temperature $T_r = (T_h^* + T_c^*)/2$, and viscous speed $u_r = \mu_r/(\rho_r H)$. All properties of the fluid are made dimensionless using their respective values at the reference temperature. Note that since we assume that the channel is open to the atmosphere, the total mass of the fluid in the channel in general can change with time. The inlet–outlet conditions for the problem can be of two types: fixed average longitudinal pressure gradient or fixed average mass flux through the channel. Let us assume that away from the ends the flow is periodic in the longitudinal direction with wavelength λ. Then, the dynamic pressure gradient averaged over the cross-section is

$$\overline{\frac{\partial \Pi}{\partial y}} = \int_0^1 \frac{\partial \Pi}{\partial y}\,\mathrm{d}x = \frac{\partial}{\partial y}\left(\int_0^1 \Pi\,\mathrm{d}x\right) = \frac{\partial \overline{\Pi}}{\partial y}, \tag{7}$$

where the overbar denotes integration over the channel width. Averaging over the wavelength in the longitudinal direction gives

$$\frac{1}{\lambda}\int_{y_0-\lambda/2}^{y_0+\lambda/2} \frac{\partial \overline{\Pi}}{\partial y}\,\mathrm{d}y \equiv \hat{\Pi} = \text{const}. \tag{8}$$

for the constant average pressure gradient case. Consequently, we can write

$$\Pi(x, y) = (\text{const} + \hat{\Pi}\, y) + \Pi'(x, y), \tag{9}$$

where Π' is periodic in the y-direction. For the case of constant mass flux, condition (8) is replaced by

$$\frac{1}{\lambda}\int_{y_0-\lambda/2}^{y_0+\lambda/2} \overline{\rho v}\, \mathrm{d}y \equiv \dot{m} = \text{const}. \tag{10}$$

The first of these two conditions generally leads to an unknown mass flux through the channel when the disturbances modify the primary flow, while the second condition leads to a variation of an unknown average vertical pressure gradient $\hat{\Pi}$ associated with the development of the secondary flow. The latter situation is somewhat similar to the flow in a closed cavity where in that case $\dot{m} \equiv 0$ (see Suslov & Paolucci 1997), although in the open channel the mass flux generally is not zero for non-Boussinesq conditions.

The dimensionless parameters appearing in the equations are respectively the Grashof number, the temperature difference, and the Prandtl number:

$$Gr = \frac{\rho_r^2 \beta_r g \Delta T H^3}{\mu_r^2}, \quad \epsilon = \frac{1}{2}\beta_r \Delta T, \quad Pr = \frac{\mu_r c_{pr}}{k_r}, \tag{11}$$

where β_r is the coefficient of thermal expansion evaluated at the reference temperature. Another dimensionless parameter entering the system through the inflow–outflow boundary conditions is the Reynolds number

$$Re = \frac{\rho_r U_r H}{\mu_r}. \tag{12}$$

It is associated with the characteristic longitudinal velocity

$$U_r = -\frac{H^2}{12\mu_r}\hat{\Pi}^*, \tag{13}$$

induced by the imposed pressure gradient $\hat{\Pi}^*$ when the constant pressure gradient case is considered. Alternatively the characteristic speed is given by

$$U_r = \frac{\dot{m}^*}{\rho_r H} - \frac{\overline{\rho^* v^*}}{\rho_r H}, \tag{14}$$

when the mass flux is fixed. Definitions (13) and (14) result in identical values only in the Boussinesq limit when the fluid density is constant. Thus, in non-Boussinesq regimes when the fluid density varies across the channel the two definitions of U_r lead to two different values of the Reynolds number for the same flow. This is also discussed in Suslov & Paolucci (1995*b*).

We assume that the working fluid in our problem is air with a reference temperature $T_r = 300\,\mathrm{K}$. The air obeys the ideal gas equation of state and the Sutherland laws for the transport properties:

$$\rho = \frac{1}{T}, \quad \mu = \frac{1 + S_\mu}{T + S_\mu} T^{3/2}, \quad k = \frac{1 + S_k}{T + S_k} T^{3/2}, \tag{15}$$

where, according to White (1974), $S_\mu = S_\mu^*/T_r = 0.368$, $S_k = S_k^*/T_r = 0.648$. We also take $c_p = 1$ (see discussion in Suslov & Paolucci 1995*a*) and $Pr = 0.71$.

3. Expansions and resulting equations

In our previous work (Suslov & Paolucci 1997) we developed an expansion procedure and multiple-timescale analysis for the system of equations describing a Newtonian fluid with general properties. We assume that a small-amplitude periodic disturbance is superimposed on the fully developed basic flow, which is steady and does not depend on the longitudinal coordinate. We then look for the solution of the problem (1)–(6) in the separable Fourier-decomposed form (truncated at the third order in amplitude and where only the first two Fourier components are retained):

$$u(x,y,t) = u_{00}(x) + \varepsilon^2|A(t)|^2 u_{20}(x) + \{[\varepsilon A(t)(u_{11}(x) + \varepsilon^2|A(t)|^2 u_{31}(x))E + \varepsilon^2 A^2(t) u_{22}(x)E^2] + \text{c.c.}\}, \tag{16}$$

$$v(x,y,t) = v_{00}(x) + \varepsilon^2|A(t)|^2 v_{20}(x) + \{[\varepsilon A(t)(v_{11}(x) + \varepsilon^2|A(t)|^2 v_{31}(x))E + \varepsilon^2 A^2(t) v_{22}(x)E^2] + \text{c.c.}\}, \tag{17}$$

$$T(x,y,t) = T_{00}(x) + \varepsilon^2|A(t)|^2 T_{20}(x) + \{[\varepsilon A(t)(T_{11}(x) + \varepsilon^2|A(t)|^2 T_{31}(x))E + \varepsilon^2 A^2(t) T_{22}(x)E^2] + \text{c.c.}\}, \tag{18}$$

$$\Pi(x,y,t) = \Pi_{00}(x) + \hat{\Pi}_{00} y + \varepsilon^2|A(t)|^2(\Pi_{20}(x) + \hat{\Pi}_{20} y) + \{[\varepsilon A(t)(\Pi_{11}(x) + \varepsilon^2|A(t)|^2 \Pi_{31}(x))E + \varepsilon^2 A^2(t)\Pi_{22}(x)E^2] + \text{c.c.}\}, \tag{19}$$

where $E = \exp(\mathrm{i}\alpha y)$ is a Fourier component of the disturbance corresponding to wavenumber α, ε is a formal parameter introduced to facilitate the expansion procedure, and c.c. denotes the complex conjugate of the preceding expression in the brackets. The first subscript corresponds to the order of amplitude entering the specific term in the expansion while the second one denotes the order of the Fourier component E. The terms $\hat{\Pi}_{m0} y$ in the expansion for the dynamic pressure are necessary in order to take into account the constant vertical pressure gradient required to maintain a fixed average mass flux through the channel when disturbances are developing. In the case of a fixed longitudinal pressure gradient $\hat{\Pi}_{00} = \hat{\Pi}$ and $\hat{\Pi}_{m0} = 0$ for $m > 0$. If we introduce the property vector $\boldsymbol{g} = (\rho, c_p, \mu, k)^T$, it can be expanded similarly:

$$\boldsymbol{g} = \boldsymbol{g}_{00}(x) + \varepsilon^2|A|^2 \boldsymbol{g}_{20}(x) + \{[\varepsilon A(\boldsymbol{g}_{11}(x) + \varepsilon^2|A|^2 \boldsymbol{g}_{31}(x))E + \varepsilon^2 A^2 \boldsymbol{g}_{22}(x)E^2] + \text{c.c.}\}, \tag{20}$$

where the components of $\boldsymbol{g}_{00}(x) = \boldsymbol{g}(T_{00}(x))$ correspond to the fluid properties of the basic flow,

$$\left.\begin{aligned} \boldsymbol{g}_{11} &= \boldsymbol{g}_{00T} T_{11}, \\ \boldsymbol{g}_{20} &= \boldsymbol{g}_{00T} T_{20} + \boldsymbol{g}_{00TT}|T_{11}|^2, \\ \boldsymbol{g}_{22} &= \boldsymbol{g}_{00T} T_{22} + \tfrac{1}{2}\boldsymbol{g}_{00TT} T_{11}^2, \\ \boldsymbol{g}_{31} &= \boldsymbol{g}_{00T} T_{31} + \boldsymbol{g}_{00TT}(T_{11}T_{20} + T_{11}^* T_{22}) + \tfrac{1}{2}\boldsymbol{g}_{00TTT} T_{11}|T_{11}|^2, \end{aligned}\right\} \tag{21}$$

and subscript T denotes partial differentiation with respect to the basic flow temperature $T_{00}(x)$ of the corresponding property variation equation. Note that, as discussed earlier, for air we take $c_p = 1$. Although for generality we include the specific heat in the expanded property vector, the actual results will be given for $c_{p00} = 1$ and $c_{p11} = c_{p20} = c_{p22} = c_{p31} = 0$. Now we assume the existence of multiple timescales so

that $A(t) = A(t_0, t_2, \ldots)$, where we take

$$t_0 = t, \quad t_2 = \varepsilon^2 t, \quad \ldots \tag{22}$$

so that

$$\frac{\partial}{\partial t} = \frac{\partial}{\partial t_0} + \varepsilon^2 \frac{\partial}{\partial t_2} + \cdots . \tag{23}$$

Note that, as shown in Suslov & Paolucci (1997), the disturbance dynamics does not depend on the first slow time $t_1 = \varepsilon t$.

Substituting expansions (16)–(19) into system (1)–(10) we obtain a set of equations at each order ε^m and for each mode E^n. Since the equations for E^n and E^{-n} are complex conjugates of each other, we limit our consideration to the equations for positive values of n. Note that $\boldsymbol{w}^*_{mn} = \boldsymbol{w}_{m-n}$.

3.1. *Basic flow equations*

At zeroth orders of ε and E we recover the basic flow equations

$$\mathrm{D}\Pi_{00} = 0, \tag{24}$$

$$\mathrm{D}(\mu_{00}\,\mathrm{D}v_{00}) - \frac{Gr}{2\epsilon}(\rho_{00} - 1) - \hat{\Pi}_{00} = 0, \tag{25}$$

$$\mathrm{D}(k_{00}\,\mathrm{D}T_{00}) = 0, \tag{26}$$

$$\mathrm{D}(\rho_{00}u_{00}) = 0, \tag{27}$$

$$u_{00} = v_{00} = 0, \quad T_{00} = 1 \pm \epsilon \quad \text{at} \quad x = 0, 1, \tag{28}$$

$$\rho_{00} = \frac{1}{T_{00}}, \quad c_{p00} = 1, \quad \mu_{00} = \left(\frac{1 + S_\mu}{T_{00} + S_\mu}\right) T_{00}^{3/2}, \quad k_{00} = \left(\frac{1 + S_k}{T_{00} + S_k}\right) T_{00}^{3/2}, \tag{29}$$

and

$$\begin{cases} \hat{\Pi}_{00} = \hat{\Pi} = -12Re & \text{if the pressure gradient is fixed,} \\ \overline{\rho_{00}v_{00}} = \dot{m} = Re & \text{if the mass flux is fixed,} \end{cases} \tag{30}$$

where $\mathrm{D} \equiv \mathrm{d}/\mathrm{d}x$. Note that integration of the x-momentum equation gives $\Pi_{00} = \text{const}$. Detailed discussions of the basic flow solution and necessary conditions for its existence are given in Chenoweth & Paolucci (1985, 1986) and Suslov & Paolucci (1995*b*). Equations (24)–(30) are solved numerically using a Chebyshev collocation spatial discretization (see Suslov & Paolucci 1995*a*, *b* for details and comparison with the analytical solution). From here on, it is implicitly understood that all operators which are obtained and discussed in subsequent sections are spatially discretized using the same Chebyshev collocation method.

3.2. *Linear disturbances*

At order $\varepsilon^1 E^1$ we obtain the linear disturbance equations, which can be given in vector form as

$$\left(A\boldsymbol{A}_\alpha - \frac{\partial A}{\partial t_0}\boldsymbol{B}\right)\boldsymbol{w}_{11} = 0, \tag{31}$$

where $\boldsymbol{w}_{11} = (u_{11}, v_{11}, T_{11}, \Pi_{11})^T$, $u_{11} = v_{11} = T_{11} = 0$ at $x = 0, 1$, and the elements of $\boldsymbol{A}_\alpha$ and $\boldsymbol{B}$ are given in Suslov & Paolucci (1997). This system of linear differential equations has a solution of the form $A\boldsymbol{w}_{11}$, where $A = \tilde{A}(t_0, t_2, \ldots)\,\mathrm{e}^{i\sigma^I t_0}$, $\tilde{A}$ satisfies the

linear equation

$$\frac{\partial \tilde{A}}{\partial t_0} = \sigma^R \tilde{A}, \tag{32}$$

and $\sigma = \sigma^R + \mathrm{i}\sigma^I$ and $\boldsymbol{w}_{11}$ are respectively complex eigenvalues and eigenvectors of the generalized eigenvalue problem

$$(\boldsymbol{A}_\alpha - \sigma \boldsymbol{B})\boldsymbol{w}_{11} = 0. \tag{33}$$

Eigensystem (33) was solved for a wide range of ϵ, Gr, and Re in Suslov & Paolucci (1995*b*). Here we normalize the eigenvectors in such a way that

$$\max |v_{11}| = \max |v_{00}|. \tag{34}$$

For the purpose of further simplification we redefine $E(y) = \exp(\mathrm{i}\alpha y) \to E(y, t_0) = \exp[\mathrm{i}\alpha(y - c_{11}t_0)]$, where $c_{11} = -\sigma^I/\alpha$ is the linear disturbance wave speed, and consequently, we then have $\tilde{A} \to A$.

The discrete system (33) is an algebraic eigenvalue problem. It is convenient to define the corresponding matrix operator $\boldsymbol{L}_{\alpha,\sigma} \equiv \boldsymbol{A}_\alpha - \sigma \boldsymbol{B}$ and its adjoint $\boldsymbol{L}^\dagger_{\alpha,\sigma} \equiv (\boldsymbol{A}^*_\alpha - \sigma^* \boldsymbol{B}^*)^T$ (stars denote complex conjugates) such that

$$\boldsymbol{L}^\dagger_{\alpha,\sigma} \boldsymbol{w}^\dagger_{11} = 0, \tag{35}$$

with $\boldsymbol{w}^\dagger_{11} = (u^\dagger_{11}, v^\dagger_{11}, T^\dagger_{11}, \Pi^\dagger_{11})^T$ and $u^\dagger_{11} = v^\dagger_{11} = T^\dagger_{11} = 0$ at $x = 0, 1$, where $\boldsymbol{w}^\dagger_{11}$ is the discrete adjoint eigenvector normalized in such a way that

$$\langle \boldsymbol{w}^\dagger_{11}, \boldsymbol{B}\boldsymbol{w}_{11} \rangle = 1. \tag{36}$$

The inner product of two discrete N-component vectors $\boldsymbol{a}$ and $\boldsymbol{b}$, denoted by angle brackets, is defined as $\langle \boldsymbol{a}, \boldsymbol{b} \rangle \equiv \sum_{i=1}^{N} a_i^* b_i$.

3.3. *Mean flow correction*

The order-$\varepsilon^2 E^0$ terms contribute to the mean flow correction. The corresponding system of equations can be written as

$$\left(|A|^2 \boldsymbol{A}_0 + \frac{\partial |A|^2}{\partial t_0} \boldsymbol{B} \right) \boldsymbol{w}_{20} = |A|^2 \boldsymbol{f}_{20}. \tag{37}$$

The mean flow correction equation must be treated differently for the two physically different situations corresponding to fixed average vertical pressure gradient and fixed average mass flux. In the first case we have $\hat{\Pi}_{20} = 0$, while in the second case we generally have a non-zero pressure gradient $\hat{\Pi}_{20}$, the magnitude of which is implicitly defined by the constant mass flux condition $\dot{m}_{20} = 0$, where

$$\dot{m}_{20} \equiv |A|^2 (\overline{\rho_{20} v_{00}} + \overline{\rho_{00} v_{20}} + 2\overline{\mathrm{Re}\{\rho_{11} v^*_{11}\}}), \tag{38}$$

and $\mathrm{Re}\{\cdot\}$ denotes the real part of the expression. Next, we note that since the channel is open, the thermodynamic pressure inside the channel is in equilibrium with that outside under low-Mach-number conditions (here we take the outside pressure to be constant). This can be the case only if the total mass of the fluid inside is allowed to vary as the disturbance develops. In fact, the amount of fluid which escapes or enters the channel portion corresponding to the disturbance wavelength $\lambda = 2\pi/\alpha$ has to be

$$M(t) - M_0 = \int_{y_0 - \lambda/2}^{y_0 + \lambda/2} [\overline{\rho(t, x, y)} - \overline{\rho_{00}(x)}] \, \mathrm{d}y = |A(t)|^2 \lambda \overline{\rho_{20}(x)} + O(|A(t)|^3), \tag{39}$$

where M_0 is the initial mass of the fluid in the same channel portion. Since the disturbance density is a function of temperature only, and the temperature distribution symmetry is broken under the non-Boussinesq conditions, the above expression is not zero in general. The fluid can escape or enter the channel through the inlet or outlet as well as in the spanwise directions if the flow between two plates is considered. This is possible only if, during the transient period, $\partial v_{20}/\partial y \neq 0$ and/or the transverse disturbance velocity w_{20} is not zero, while these terms must vanish when the quasi-steady state is again reached. Thus, when disturbances develop, the flow in an open channel cannot be represented by the expansions (16)–(20). On other hand, the weakly nonlinear theory of a selected disturbance mode, by its very nature, only tells us about the asymptotic long-time behaviour of the flow. The only long lasting effect of the transient development which we must take into account is the permanent fluid mass change in the flow domain. To accomplish this we introduce the spatially uniform mass source term $|A|^2 S_{\rho 20}$ into the continuity equation so that at the order considered it becomes

$$\frac{\partial |A|^2}{\partial t_0}(\rho_{20} + S_{\rho 20}) + |A|^2 \,\mathrm{D}(\rho_{00} u_{20} + 2\mathrm{Re}\,\{\rho_{11} u_{11}^*\}) = 0. \tag{40}$$

Integrating (40) over the channel width and taking into account the no-slip no-penetration boundary conditions we obtain

$$\frac{\partial |A|^2}{\partial t_0}(\overline{\rho_{20}} + S_{\rho 20}) = 0 \tag{41}$$

or

$$S_{\rho 20} = -\overline{\rho_{20}} = \frac{M_0 - M(t)}{|A(t)|^2 \lambda} + O(|A(t)|). \tag{42}$$

In order to justify the spatial uniformity of the mass source term, we note that any local temperature change leads to an instantaneous change in the local thermodynamic pressure. This causes acoustic waves to propagate at a speed which is assumed to be much greater than the characteristic speed of the fluid inside the channel. Indeed, in the low-Mach-number approximation, the acoustic speed is infinite. Thus, the acoustic disturbance reaches the inlet, outlet or spanwise openings instantly and causes a fast fluid discharge or inflow such that the thermodynamic pressure inside the channel equilibrates with the ambient one. Physically, the characteristic time necessary for the acoustic disturbance to reach the end of the channel is L/a, where L is the channel length and $a = \sqrt{\gamma_r R T_r}$ is the reference sound speed. On other hand, the characteristic time for the disturbance development is $(H/u_r)/|\sigma^R|$. Thus, in order to justify the introduction of the spatially uniform mass source term, we need to have

$$\frac{L}{a} \ll \frac{H/u_r}{|\sigma^R|} \tag{43}$$

or

$$|\sigma^R|\eta \ll \frac{1}{Ma}, \tag{44}$$

where $\eta = L/H$ is the channel aspect ratio, and $Ma = u_r/a$ is the reference Mach number. The estimate for a fully developed flow for $\eta \simeq 40$ in a channel of width $H = 10\,\mathrm{cm}$ at $T_r = 300\,\mathrm{K}$ gives $|\sigma^R| \ll 5.7 \times 10^2$. For all computed results we find $|\sigma^R| \ll 10^2$. Thus the approximation of a spatially uniform mass source is very good for the flow considered.

The necessity of a spatially uniform mass source term when the low-Mach-number

equations are used to describe the flow in an open system was first recognized in Fröhlich, Laure & Peyret (1992), although there the source term was introduced only in the continuity equation. Apparently that led to inconsistent momentum and energy equations. If one proceeds consistently from the complete set of equations (1)–(3) written in conservative form, then one needs to include additional convective terms in the momentum and thermal energy equations. The resulting equations in operator form are

$$\boldsymbol{L}_{0,\,2\sigma^R}\boldsymbol{w}_{20} = \boldsymbol{F}_{20}, \tag{45}$$

where $\boldsymbol{w}_{20} = (u_{20}, v_{20}, T_{20}, \Pi_{20})^T$, $u_{20} = v_{20} = T_{20} = 0$ at $x = 0, 1$, $\boldsymbol{F}_{20} = \boldsymbol{f}_{20} - 2\sigma^R S_\rho \boldsymbol{f}_{20}$, the expressions for $\boldsymbol{f}_{20} = (f_{20}^{(1)},\ f_{20}^{(2)},\ f_{20}^{(3)},\ f_{20}^{(4)})^T$ are given in the Appendix, and $\boldsymbol{f}_{20} = (u_{00}, v_{00}, c_{p00}T_{00}, 1)^T$. The detailed solutions of (45) for a wide range of governing parameters are presented in Part 2 (Suslov & Paolucci 1999).

Note that at this order, equation (45) is real since all terms involving the imaginary parts drop out identically.

3.4. *Periodic second-order terms*

Collecting terms of order $\varepsilon^2 E^2$, we obtain

$$\boldsymbol{L}_{2\alpha,\,2\sigma}\boldsymbol{w}_{22} = \boldsymbol{f}_{22}, \tag{46}$$

where $\boldsymbol{w}_{22} = (u_{22}, v_{22}, T_{22}, \Pi_{22})^T$, $u_{22} = v_{22} = T_{22} = 0$ at $x = 0, 1$, and the components of $\boldsymbol{f}_{22} = (f_{22}^{(1)},\ f_{22}^{(2)},\ f_{22}^{(3)},\ f_{22}^{(4)})^T$ are given in Suslov (1997).

Note that the equations for the mean flow correction (45) and the second harmonic (46) can be easily solved for non-resonant conditions. A derivation of the resonance conditions and detailed discussion of the resonances arising at second order in amplitude are given in Suslov & Paolucci (1997).

3.5. *Amplitude equation*

When the disturbance amplitude is very small, it varies exponentially with time. In order to assess the possible saturation when the amplitude becomes finite, we proceed to examine the system, which results at order $\varepsilon^3 E^1$ in

$$A|A|^2(\boldsymbol{L}_{\alpha,\,\sigma} - 2\sigma^R\boldsymbol{B})\boldsymbol{w}_{31} = \frac{\partial A}{\partial t_2}\boldsymbol{B}\,\boldsymbol{w}_{11} + A|A|^2\boldsymbol{F}_{31}, \tag{47}$$

where $\boldsymbol{w}_{31} = (u_{31}, v_{31}, T_{31}, \Pi_{31})^T$, $u_{31} = v_{31} = T_{31} = 0$ at $x = 0, 1$, $\boldsymbol{F}_{31} = \boldsymbol{f}_{31} - 2\sigma^R S_\rho \boldsymbol{f}_{31}$, the components of the vector $\boldsymbol{f}_{31} = (f_{31}^{(1)}, f_{31}^{(2)}, f_{31}^{(3)}, f_{31}^{(4)})^T$ are given in Suslov (1997), and $\boldsymbol{f}_{31} = (u_{11}, v_{11}, c_{p00}T_{11} + c_{p11}T_{00}, 0)^T$. Considering the inner product of (47) with $\boldsymbol{w}_{11}^\dagger$ and using (36) we obtain

$$-2\sigma^R\tilde{K}_0 A|A|^2 = \frac{\partial A}{\partial t_2} + \tilde{K}_1 A|A|^2, \tag{48}$$

where

$$\tilde{K}_0 = \langle \boldsymbol{w}_{11}^\dagger, \boldsymbol{B}\,\boldsymbol{w}_{31}\rangle, \quad \tilde{K}_1 = \langle \boldsymbol{w}_{11}^\dagger, \boldsymbol{F}_{31}\rangle. \tag{49}$$

Since the left-hand side and the second term on the right-hand side of (48) have a similar structure, subsequently we must have that

$$\frac{\partial A}{\partial t_2} = K_1 A|A|^2, \tag{50}$$

where K_1 is the Landau constant. If $\sigma^R \to 0$, then the left-hand side of (48) vanishes and thus we must have

$$K_1 \to -\tilde{K}_1. \tag{51}$$

This is the conventional solvability condition. Whenever the flow is considered away from the marginal stability surface ($\sigma^R \neq 0$), the left-hand side of (48) does not vanish and remains unknown. In this case, as shown in Suslov & Paolucci (1997), the proper choice of the first Landau constant is determined by the orthogonality condition $\langle \boldsymbol{w}_{11}, \boldsymbol{w}_{31} \rangle = 0$ and is given by

$$K_1 = -2\sigma^R \frac{\langle \boldsymbol{w}_{11}, \boldsymbol{\chi} \rangle}{\langle \boldsymbol{w}_{11}, \boldsymbol{w}_{11} \rangle}, \tag{52}$$

where $\boldsymbol{\chi} = (u_\chi, v_\chi, t_\chi, \Pi_\chi)^T$ is the solution of the supplementary problem

$$(\boldsymbol{L}_{\alpha,\sigma} - 2\sigma^R \boldsymbol{B})\boldsymbol{\chi} = \boldsymbol{F}_{31} \tag{53}$$

with boundary conditions $u_\chi = v_\chi = T_\chi = 0$ at $x = 0, 1$.

Now reconstituting the time derivative of the amplitude using (23), (32) and (50) we have

$$\frac{\partial A}{\partial t} = \frac{\partial A}{\partial t_0} + \varepsilon^2 \frac{\partial A}{\partial t_2} + \cdots = \sigma^R A + \varepsilon^2 K_1 A|A|^2 + \cdots . \tag{54}$$

Since ε is just a formal order parameter we redefine $\varepsilon A \to A$ and, neglecting the higher-order terms in amplitude, we obtain the cubic Landau equation for the disturbance amplitude $A = A(t)$

$$\frac{\partial A}{\partial t} = \sigma^R A + K_1 A|A|^2. \tag{55}$$

The equilibrium amplitudes are $A_e = 0$ and $|A_e|^2 = a_e^2 = -\sigma^R / K_1^R > 0$, where in polar form $A = a\,\mathrm{e}^{\mathrm{i}\theta}$. It is easy to show that (55) provides a stable finite amplitude only for the case of supercritical bifurcation ($K_1^R < 0$). In the case of subcritical bifurcation ($K_1^R > 0$) at least a fifth-order Landau equation must be derived to predict a stable equilibrium disturbance amplitude.

4. Results

All numerical results were obtained using 50 spectral modes (see Suslov & Paolucci 1995*b* for a description of the numerical approximation) and double-precision versions of appropriate IMSL routines (IMSL 1989): NEQNF to solve for the basic flow, GVCCG and GVLRG to solve the generalized eigenvalue problem for $\alpha > 0$ and $\alpha = 0$ respectively, LSBRR to solve the mean flow correction equations, and LSACG to solve equations for the second harmonic and for $\boldsymbol{\chi}$.

4.1. *Bifurcations*

The cubic Landau equation predicts an equilibrium disturbance amplitude if the flow bifurcates supercritically. In the case of a subcritical bifurcation the Landau equation provides some useful information about the disturbance dynamics while the amplitude is sufficiently small, but in general cannot provide any information about the saturation state unless a fifth-order term in amplitude is included and its coefficient has the proper sign. Otherwise still higher orders would be required to obtain the equilibrium state. Since the derivation and analysis of higher-order Landau equations is beyond the scope of the present work, first we establish ranges

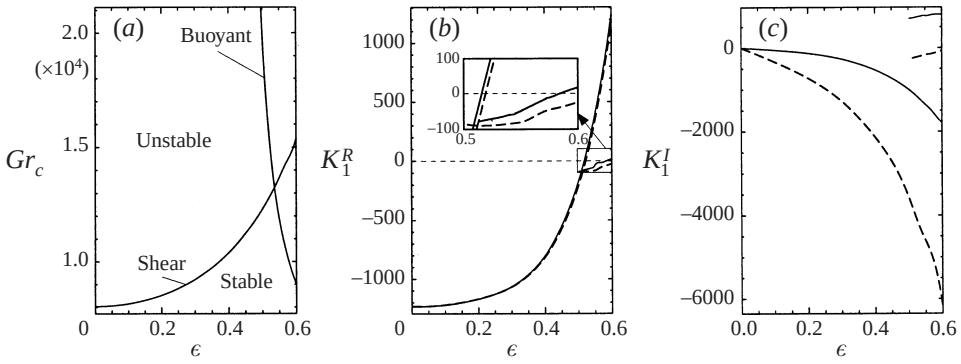

FIGURE 1. (*a*) Critical Grashof number, and (*b*) real and (*c*) imaginary parts of the first Landau constant as functions of ϵ evaluated at $Gr = Gr_c(\epsilon)$ for $Re = 0$. Solid and dashed lines in (*b*) and (*c*) represent cases with $\partial\overline{\Pi}/\partial y = 0$ and $\dot{m} = 0$ conditions, respectively.

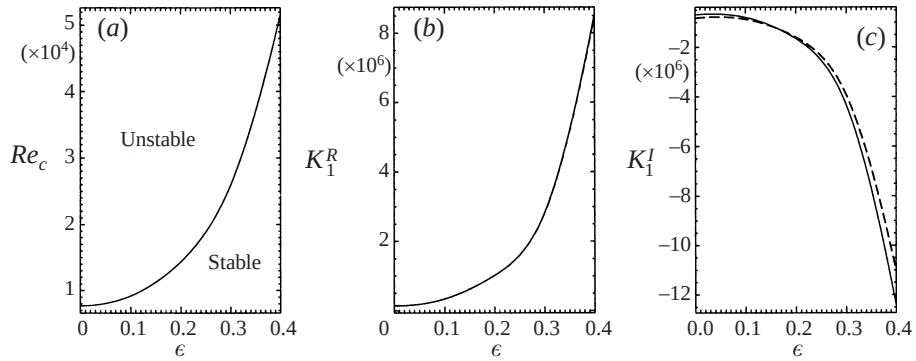

FIGURE 2. (*a*) Critical Reynolds number and (*b*) real and (*c*) imaginary parts of the first Landau constant as functions of ϵ evaluated at $Re = Re_c(\epsilon)$ for $Gr = 0$. Solid and dashed lines in (*b*) and (*c*) represent cases with $\partial\overline{\Pi}/\partial y = \text{const}$ and $\dot{m} = \text{const}$ conditions, respectively.

of Reynolds number where the bifurcation is supercritical and thus the cubic Landau equation can be used to estimate the equilibrium amplitude. In order to do this, we look at the real part of the first Landau constant K_1 evaluated for different values of Gr, Re, and ϵ. Note that the actual value of K_1 changes as we move away from criticality and, strictly speaking, it has to be computed for each set of parameters $(Re, Gr, \epsilon; \alpha)$. On other hand, our investigation shows that the qualitative character of the results presented below remains the same for substantial distances away form the critical points (at least up to $|\delta| = 0.2$, where $\delta \equiv P/P_c - 1$, P represents a governing parameter, typically Re or Gr, and the subscript c denotes the critical value).

The first Landau constant for $Re = 0$ (natural convection) is presented in figures 1(*b*) and 1(*c*) as a function of ϵ for $Gr = Gr_c(\epsilon)$ which is shown in figure 1(*a*). The picture is quite similar to the one presented for convection in a closed cavity (see Suslov & Paolucci 1997); that is, for the shear mode, $K_1^R < 0$ up to $\epsilon \approx 0.536$ predicting the existence of a supercritical bifurcation. One can notice the slight difference in the behaviour of the first Landau constant for the buoyant mode at higher values of ϵ: its real part becomes positive for ϵ slightly below 0.6 while it is always negative for the closed cavity in the parameter range considered. The major physical difference between flows in a closed cavity and an open channel is that in the latter case the fluid

	Sen & Venkateswarlu			Present results	
$(3/4)Re$	Method	$-K_1^I/K_1^R$	$(\sigma^R/\sigma^I)\times 10^3$	$-K_1^I/K_1^R$	$(\sigma^R/\sigma^I)\times 10^3$
5200	W RP	5.311 5.105	4.01	5.188	4.00
5400	W RP	5.488 5.039	2.52	5.421	2.50
5500	W RP	5.586 4.987	1.81	5.550	1.79
5625	W RP	9.211 4.923	0.80	10.965	0.78
5700	W RP	4.230 4.901	0.47	4.274	0.46
5710	W RP	4.432 4.898	0.41	4.456	0.40
5720	W RP	4.566 4.895	0.35	4.585	0.33
5730	W RP	4.660 4.888	0.29	4.675	0.27
5750	W RP	4.784 4.878	0.16	4.794	0.14
5774	W RP	4.867 4.868	0.01	4.881	−0.01

TABLE 1. Comparison of selected results for subcritical Poiseuille flows ($\epsilon = 10^{-5}$, $Gr = 0$, $\alpha = 2.04$) with computations of Sen & Venkateswarlu (1983). W stands for Watson's 'true problem' and RP for Reynolds & Potter's 'false problem' approaches.

can enter the channel or discharge from it as disturbances develop. Consequently, removal of the global mass conservation constraint in the natural convection flow in an open channel leads to the appearance of a subcritically bifurcating buoyant instability mode in highly non-Boussinesq regimes. Note that in the Boussinesq limit $\epsilon \to 0$, consistent with previous works (Mizushima & Gotoh 1983; Fujimura & Mizushima 1987), $K_1^I \to 0$ meaning that growing disturbances remain stationary (and symmetric) when the temperature difference between the walls approaches zero. Note also that in the Boussinesq limit the open channel results for fixed pressure gradient and fixed mass flux cases are identical because of the symmetries of the basic flow and disturbance distributions across the channel. Additionally, when $Re = 0$ the results are identical to those obtained in the Boussinesq limit for natural convection flow in a tall enclosure (Suslov & Paolucci 1997).

Values of the first Landau constant for forced convection flow (Poiseuille-type flow, $Gr = 0$) are presented in figures 2(b) and 2(c) for different values of ϵ and $Re = Re_c(\epsilon)$ which is shown in figure 2(a). Note that the actual values of the Landau constant depend on the chosen normalization (see (34)) and cannot be compared directly to results of other authors. On other hand, the ratio K_1^I/K_1^R is invariant with respect to any normalization. This ratio provides an accuracy check for our numerical results. For the critical point $(Gr_c, Re_c, \alpha_c) \approx (0, 7696.3, 2.0411)$ for Poiseuille flow in the Boussinesq limit $\epsilon \to 0$ (here we take $\epsilon = 10^{-5}$) in the case of fixed pressure gradient, we obtain $K_1^I/K_1^R = -4.8416$ which is reasonably close to the value of -4.87 reported by Sen & Venkateswarlu (1983). Similar ratios given in the literature

(Reynolds & Potter 1967; Davey, Hocking & Stewartson 1974; Fujimura 1989) for the case of fixed mass flux range from -5.62 up to -5.58. To the authors' knowledge, the most accurate value obtained in this case is that of Fujimura (1989) who gives $K_1^I/K_1^R = -5.5832$. Our value of $K_1^I/K_1^R = -5.5838$ is in very close agreement with his result. Our results also compare favourably with those of Sen & Venkateswarlu (1983) for subcritical Poiseuille flow as can be seen from table 1. Owing to a different non-dimensionalization, our values for Re and α are larger than theirs by factors of $4/3$ and 2, respectively. Note that the results for the linear eigenvalue problem presented in Sen & Venkateswarlu (1983) seem to be slightly inaccurate since the value of the critical Reynolds number for the Poiseuille flow ($Re_c \approx 5772$ when the non-dimensionalization is based on maximum speed and half of the channel width) is apparently overestimated. As a consequence, our eigenvalue results (σ^R/σ^I in table 1) are presumably more accurate but differ slightly from the ones obtained by Sen & Venkateswarlu.

The values obtained for the first Landau constant ($-K_1^I/K_1^R$) generally lie between similar values obtained by Sen & Venkateswarlu using Watson's (1960) 'true problem' and Reynolds & Potter's (1967) false problem techniques. Note that Watson's approach leads to a singular behaviour in the vicinity of the subcritical Reynolds number value of 7533 (or $3Re/4 = 5650$). Here a resonance between the mean flow correction induced by the fundamental mode with $\alpha = 2.04$ and the $\alpha = 0$ disturbance mode occurs (see Suslov & Paolucci 1997), i.e. the condition $2\sigma^R|_{\alpha=2.04} = -\pi^2$, is satisfied, where, as can be shown in the Boussinesq limit, $\sigma_n = -(n^2\pi^2)$ and $\sigma_n = -(n^2\pi^2)/Pr$, $n = 1, 2, \ldots$ are the eigenvalues of problem (33) associated with the momentum and thermal energy equations, respectively, for $\alpha = 0$ in case of fixed pressure gradient. This type of resonance limits the applicability of the one-mode analysis of Watson in subcritical regimes (see discussions in Davey & Nguyen 1971; Herbert 1983; Sen & Venkateswarlu 1983). Although not identical, our reduction scheme is similar to Watson's method and has similar limitations (we also obtain a singularity at the resonant point, see table 1).

Note that the analysis of subcritical flows when the average mass flux is fixed is less restricted since the eigenvalues associated with the momentum equations in the Boussinesq limit at $\alpha = 0$ are $-4(n^2\pi^2)$, $n = 1, 2, \ldots$. Recently, the present authors (Suslov & Paolucci 1997) noted that this difficulty can be avoided within a 'true problem' approach by considering the interaction with the mean flow modes. This would require derivation of a system of the coupled amplitude equations and the corresponding coupled Landau series in the vicinity of the resonant point. Note that the cubic Landau equation considered in the present paper is a low-order truncation of the infinite-order Landau equation representing the temporal evolution of the disturbance amplitude. It is accurate only if this amplitude is sufficiently small. As discussed in Davey & Nguyen (1971) and Herbert (1983), when the infinite Landau series is considered for a subcritical flow with $\sigma^R < 0$, it is practically impossible to choose the governing parameters to avoid all higher-order mean flow resonances. The single-mode infinite Landau series is inevitably divergent since at least one of its coefficients becomes infinite (see figure 2*c*, *d* in Suslov & Paolucci 1997) as a reflection of inherently multimode interaction during the decay of disturbances.

Thus, in general, the infinite system of coupled Landau equations is necessary to describe adequately the physics of subcritical flows and to derive corresponding convergent Landau series. On the other hand it is relatively easy to locate the lowest-order resonant points (there exists only a finite number of them) and consider the dynamics in the parameter ranges away from them. In this case the Landau equations

would be necessary to define only the higher order Landau constants which are multiplied by higher powers of the amplitude in the infinite coupled Landau series. If the disturbance amplitude is sufficiently small, neglecting these higher-order terms in the infinite Landau series (now convergent with finite coefficients obtained from the mode coupling) would not lead to a large error. It can be shown then that the cubic Landau equation obtained by the low-order truncation of the infinite-order coupled Landau equations is identical to the one derived from a single-mode analysis discussed in detail in this paper if the first mean flow resonance occurs at the order $|A|^4$ or higher (see also discussion on page 18 in Suslov & Paolucci 1997). Thus in the present paper we will report results only for regions away from the lowest-order resonances assuming that the disturbance amplitude is small enough so that the derived cubic Landau equation is a reasonable approximation of the infinite-order coupled Landau equations. This assumption has a simple physical interpretation. While for the fundamental disturbance mode the decay rate is $\sigma^R < 0$, for the disturbance resonating with the mean flow mode it is much faster, $2m\sigma^R,\ m > 1$. In order for this resonant interaction to have a noticeable effect, the initial amplitude of the resonant mode must be large enough to persist for sufficiently long time. If the amplitude is small, then the mode decays so quickly that the contribution due to the resonance is negligible. The general indication that higher-order resonances may not affect strongly the qualitative behaviour of the solution can be found in the literature (see, for example, Glendinning 1984); however, further investigation of this theoretical aspect is required.

We should note that on the surface, the 'false problem' approach suggested by Reynolds & Potter circumvents the difficulties mentioned above and thus one is able to estimate the Landau constant in subcritical regimes. The fact that no singularities arise in this method is typically used as an argument for the superiority of this method for subcritical flows (see, for example, Sen & Venkateswarlu 1983). On other hand, the failure of Watson's approach indicates the presence of a strong mean flow interaction among the decaying disturbances, a mechanism which does not play an important role in supercritical flows. By its nature, Reynolds & Potter's approach does not take this interaction into account. As shown in Suslov & Paolucci (1997), coexistence of different disturbance modes, even in the case when their linear amplification (or decay) rates are substantially different, could lead to a stable mixed state with equilibrium amplitudes different from the ones predicted by the one-mode analysis. Moreover, the results obtained by Sen & Venkateswarlu (1983) for Poiseuille flow using Reynolds & Potter's approach are not in a good agreement with the available experimental data by Nishioka *et al.* (1975) (see the discussion in the next subsection). Thus we choose to stay with the Watson-type reduction scheme, which from our point of view retains more physical features of the original problem.

As seen from figure 2, the value of K_1^R remains positive and increases monotonically with ϵ. Thus, the forced convection flow, although substantially stabilized according to linear theory, always bifurcates subcritically, and, consequently, higher-order expansions are necessary to give an adequate Landau model for such a flow. Note that lines corresponding to the fixed average pressure gradient and to the fixed average mass flux conditions in figure 2(*b*) are very close to each other and cannot be distinguished in the figure. Figure 3 presents the results for mixed convection in the Boussinesq limit $\epsilon \to 0$ (for which $\epsilon = 0.005$ is taken in our computations). Since in the Boussinesq limit the results are symmetric with respect to the inversion of the sign of the Reynolds number, only values for $Re \geqslant 0$ are presented. From figure 3(*b*) we see that the bifurcation in the Boussinesq mixed convection flow remains supercritical along line

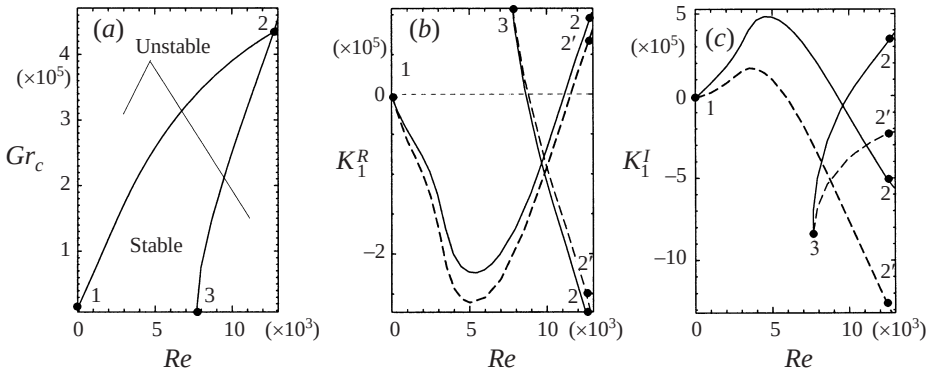

FIGURE 3. (*a*) Critical Grashof number, and (*b*) real and (*c*) imaginary parts of the first Landau constant as functions of Reynolds number for mixed convection flow in the Boussinesq limit ($\epsilon \to 0$). Solid and dashed lines in (*b*) and (*c*) represent cases with $\partial\overline{\Pi}/\partial y = \text{const}$ and $\dot{m} = \text{const}$ conditions, respectively. A discussion of the labelled points is given in the text.

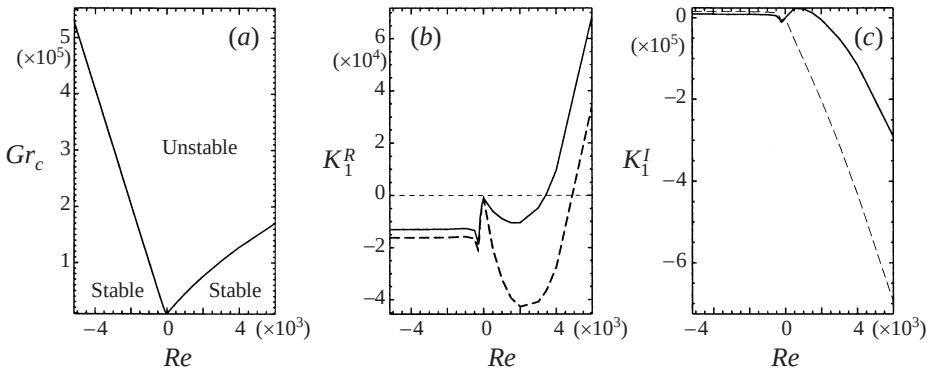

FIGURE 4. (*a*) Critical Grashof number, and (*b*) real and (*c*) imaginary parts of the first Landau constant as functions of Reynolds number for mixed convection flow in the non-Boussinesq regime with $\epsilon = 0.3$. Solid and dashed lines in (*b*) and (*c*) represent cases with $\partial\overline{\Pi}/\partial y = \text{const}$ and $\dot{m} = \text{const}$ conditions, respectively.

1–2 (point 1 represents natural convection) up to $|Re| \approx 1.12 \times 10^4$ ($|Re| \approx 1.17 \times 10^4$) when the pressure gradient (mass flux) is kept fixed. For Poiseuille-type flows (line 3–2) the situation is the opposite: the bifurcation is subcritical for purely forced convection (point 3) and changes to supercritical as the Grashof number increases. From figure 4 we see that the symmetry is completely broken in the non-Boussinesq regime at $\epsilon = 0.3$. The bifurcation remains supercritical for negative and relatively small positive Reynolds numbers and becomes subcritical for $Re \gtrsim 3400$ ($Re \gtrsim 4900$) when the force associated with the applied pressure gradient opposes the buoyancy in the region close to the cold wall, where the disturbance maximum is located (see Suslov & Paolucci 1995*b*, 1997 for details). Thus the range of Reynolds numbers where the cubic Landau equation models the complete dynamics of the disturbances adequately becomes substantially smaller when fluid properties are allowed to vary with temperature.

From figures 1–4 we notice that for fixed ϵ and Re the value of $|K_1^R|$ obtained for the case of fixed average pressure gradient is generally smaller than the corresponding value for the case of fixed average mass flux. Since the magnitude of the equilibrium

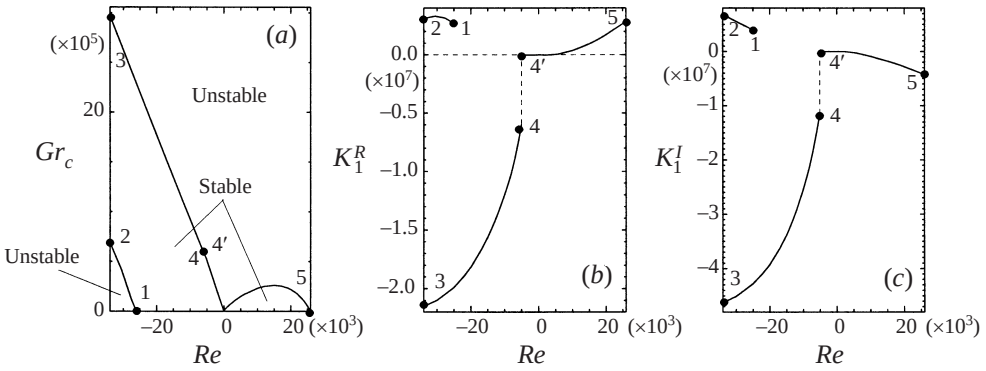

FIGURE 5. (*a*) Critical Grashof number, and (*b*) real and (*c*) imaginary parts of the first Landau constant as functions of Reynolds number for mixed convection flow in the non-Boussinesq regime with $\epsilon = 0.3$ for a larger Reynolds number range in the case with $\partial\overline{\Pi}/\partial y = \text{const}$. A discussion of the labelled points is given in the text.

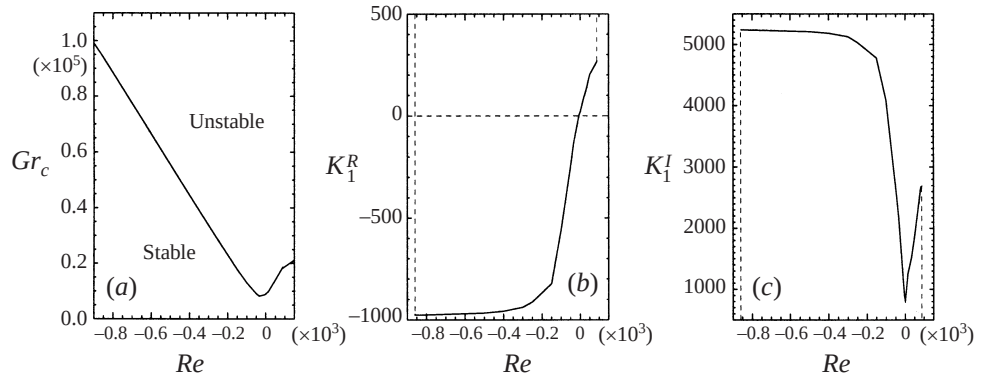

FIGURE 6. (*a*) Critical Grashof number, and (*b*) real and (*c*) imaginary parts of the first Landau constant as functions of Reynolds number for mixed convection flow in the non-Boussinesq regime with $\epsilon = 0.6$ in the case with $\partial\overline{\Pi}/\partial y = \text{const}$. Dotted vertical lines in (*b*) and (*c*) show the locations of codimension-2 points.

disturbance amplitude is inversely proportional to $|K_1^R|^{1/2}$ we conclude that fixing the pressure gradient is slightly less constraining than fixing the mass flux in the sense that disturbances should be more easily observable in the former case. Otherwise, the results for both cases are similar. Thus, in further discussions we limit ourselves primarily to the fixed pressure gradient case. In figure 5 we show values of the first Landau constant for the case of fixed pressure gradient and $\epsilon = 0.3$ for a much larger Reynolds number range. Note that the shear instability mode which becomes dominant for $Re \lesssim -5180$ (see Suslov & Paolucci 1995*b*) always bifurcates supercritically (line 3–4 in figure 5*b*). Since the corresponding value of $|K_1^R|$ is several orders of magnitude larger than the value for the shear mode which is dominant when $Re \gtrsim -5180$ (line 4′–5 in figure 5*b*), it is expected that the former mode will have a much smaller amplitude in the vicinity of the codimension-2 point 4–4′ where the two modes become unstable simultaneously. No regions of supercritical bifurcations are found for larger positive Reynolds numbers (in the vicinity of point 5) or for Poiseuille-type flows (lines 1–2 in figure 5) which become linearly unstable for substantially higher values of $|Re|$ owing to the fluid properties variations as

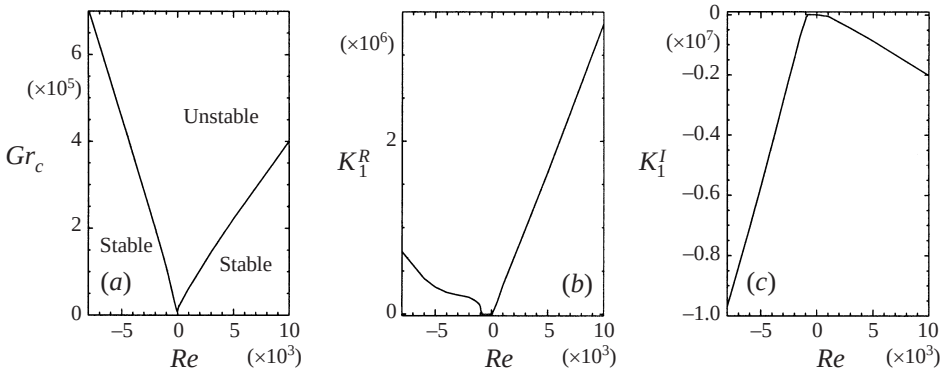

FIGURE 7. (*a*) Critical Grashof number, and (*b*) real and (*c*) imaginary parts of the first Landau constant as functions of Reynolds number for mixed convection flow in the non-Boussinesq regime with $\epsilon = 0.6$ for a larger Reynolds number range in the case with $\partial\overline{\Pi}/\partial y = \text{const}$.

discussed in Suslov & Paolucci (1995*b*). Note also that points 1 and 5 in figure 5 are equivalent to each other since they represent the same purely forced flow profiles ($Gr = 0$), but with velocities in opposite directions.

In the strongly non-Boussinesq regime with $\epsilon = 0.6$, the buoyant instability mode discussed in Suslov & Paolucci (1995*b*) bifurcates supercritically for $Re \lesssim -10$. As seen from figure 6, this range covers a substantial part of the region where, according to linear theory, it dominates the shear-driven instability. The shear mode always bifurcates subcritically as seen from figure 7. Note that lines similar to 2–3 in figure 3 and 1–2 in figure 5 which correspond to dominant forced convection are not presented in figures 6 and 7 since the linear instability in this case occurs at extremely large Reynolds numbers (see figure 2 and Suslov & Paolucci 1995*b*). Summarizing, we conclude that the non-Boussinesq effects have a strong influence on the stability characteristics of the primary flow. Not only do the values of critical parameters predicted by linear stability analysis deviate substantially from the Boussinesq predictions, but also the character of bifurcation changes qualitatively as the temperature difference between the walls increases.

4.2. *Disturbance amplitudes*

While the periodic disturbances discussed in Suslov & Paolucci (1995*b*) and mean flow correction distributions (see Part 2) represent the spatial form of the flow fields beyond the bifurcation, they do not provide any information on the actual size of the disturbances or on how the disturbances develop. Thus in this section we analyse the solutions for the disturbance amplitude satisfying the Landau equation (55). The current reduction scheme enabled us to derive the Landau equation which governs the dynamics of the disturbance amplitude away from the bifurcation point. Typically, in weakly nonlinear theory, when the relative distance from the critical point is taken as a small expansion parameter, the constants entering the Landau equation are evaluated at the critical point. Then the equilibrium amplitude for a disturbance wave is estimated as

$$\left|\frac{\sigma^R(\delta)}{K_1^R(\delta=0)}\right|^{1/2}, \quad \text{where } \delta = (Re/Re_c - 1)\Big|_{\epsilon,\, Gr \text{ fixed}} \quad \text{or} \quad \delta = (Gr/Gr_c - 1)\Big|_{\epsilon,\, Re \text{ fixed}}$$

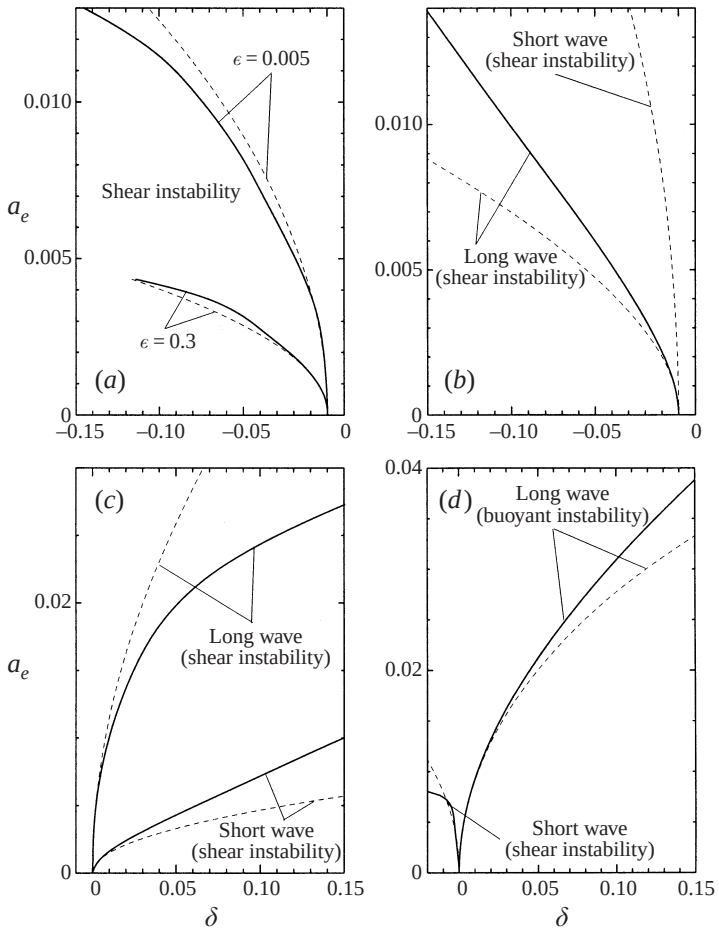

FIGURE 8. Bifurcation diagrams for disturbance waves for $\partial\overline{\Pi}/\partial y = \text{const}$ and (*a*) Poiseuille-type flows $(\epsilon, Re, Gr) = (0.005, 7700, 0)$ and $(\epsilon, Re, Gr) = (0.3, 25960, 0)$, and codimension-2 points at (*b*) $(\epsilon, Re, Gr) = (0.005, 12850, 442730)$, (*c*) $(\epsilon, Re, Gr) = (0.3, -5150, 524640)$, and (*d*) $(\epsilon, Re, Gr) = (0.6, -860, 95032)$. Dotted lines represent the approximate bifurcation diagrams obtained using the value of the first Landau constant at the corresponding critical points ($\delta = 0$).

for Poiseuille-type flows and for natural or mixed convection flows, respectively. In this approach one implicitly assumes that the Landau constant does not change with δ. From figure 8 we see that this is not the case in general. Thus, a conclusion we draw in analysing the bifurcation diagrams in figure 8 is that one should be careful when trying to sum the higher-order terms in the Stuart–Landau series in order to predict an equilibrium amplitude away from the bifurcation point as done, for instance, in Sen & Venkateswarlu (1983). The correction due to the higher-order terms in the Stuart–Landau series in some cases can be of the same order as the error introduced when the variation of the Landau constants with δ is neglected.

The bifurcation diagrams presented in figure 8 show the equilibrium amplitudes when the bifurcations are supercritical, and the threshold amplitudes which limit the basin of attraction of the undisturbed parallel flow when the bifurcations are subcritical, both for periodic wave disturbances with wavenumbers corresponding to those of maximum linear growth rate. Values of critical parameters were found

in our earlier work on linear stability of mixed convection flow (Suslov & Paolucci 1995*b*). From figure 8(*a*) we conclude that Poiseuille-type flows become much more sensitive to the size of disturbances when the temperature difference is increased since the threshold amplitude is substantially decreased. The threshold amplitude corresponding to $\epsilon = 0.3$ is difficult to obtain for larger values of $|\delta|$ because a mean flow resonance (Suslov & Paolucci 1997) occurs just beyond the curve truncation point in the figure. The situation is even worse for the mixed convection flow in the vicinity of the codimension-2 point in the Boussinesq limit (as discussed in Suslov & Paolucci 1995*b*), two different shear instability modes with $\alpha = 1.6815$ and $\alpha = 2.1074$ compete here) which is shown in figure 8(*b*): the influence of the mean flow resonance extends very close to the bifurcation point such that only the approximate values of the threshold amplitudes based on the Landau constant estimated for $\delta = 0$ are presented for the subcritically bifurcating short-wavelength instability mode. Note that although the values of δ are negative, the long-wavelength instability bifurcates supercritically ($K_1^R < 0$ as can be seen from figure 3*b*). The negative values of δ arise since the flow is destabilized when the value of the Grashof number is decreased below Gr_c (down from point 2 and below line 2–3 in figure 3*a*). Figure 8(*b*) indicates that the equilibrium long-wavelength disturbance amplitude remains smaller than the threshold amplitude for the shorter wave. This fact suggests that the longer wave should represent a stable state in the vicinity of the codimension-2 point in the Boussinesq limit, although mode coupling must be taken into account to complete the investigation of pattern selection (see Suslov & Paolucci 1997). From figure 8(*c*) we see that at $\epsilon = 0.3$ two shear modes (see Suslov & Paolucci 1995*b*) bifurcate supercritically in the vicinity of the codimension-2 point (our computations show that $K^R < 0$ at points 4 and 4′ in figure 5*b*). Again the long shear instability wave ($\alpha = 0.0800$) is expected to play a dominant role since it is characterized by a much larger equilibrium amplitude than that for the short wave ($\alpha = 1.1828$). However, this can only be confirmed by examining the coupled equations near the codimension-2 point, which is beyond the scope of the present work. The short-wave disturbance equilibrium amplitude is smaller since the dissipation is more intense for smaller cells. From figure 8(*d*) we see that in the strongly non-Boussinesq regime at $\epsilon = 0.6$, the interaction is between the shear ($\alpha = 0.6285$) and buoyant ($\alpha = 0.1000$) modes (see Suslov & Paolucci 1995*b*). For the downward flow the former is subcritical and the latter is supercritical (see figures 6*b* and 7*b*), while for the upward flow both bifurcations are subcritical. The individual bifurcation diagrams shown in figure 8(*d*) for the codimension-2 point correspond to the downward flow case. It is expected that for Grashof numbers smaller than the critical value, sufficiently large initial disturbances will lead to the shear type of instability. For larger Grashof numbers, the basic flow could initially be destabilized by buoyant disturbances which could then excite the shear instability so that finally it becomes dominant or leads to some mixed state depending on the specific choice of parameters. The codimension-2 analysis can be performed by deriving the coupled Landau equations as in Suslov & Paolucci (1997). This has not been done at this point.

Evaluations of equilibrium disturbance amplitudes are necessary in order to quantitatively predict such important characteristics of the disturbed flow as the average heat transfer rate or the average mass flux. Thus, it is instructive to compare predictions based on the proposed reduction scheme with experimental results. Unfortunately, experiments in the vicinity of criticality, where weakly nonlinear theory is most accurate, are generally very difficult to perform owing to very small and, consequently,

hard to detect deviations from the undisturbed state. One experiment where special care was taken to control accurately the disturbance amplitude was performed by Nishioka *et al.* (1975) in the subcritical Poiseuille flow. Although this relatively simple flow has been studied extensively for decades, to date attempts to predict the threshold amplitude using weakly nonlinear theory (see Sen & Venkateswarlu 1983; Zhou 1982) have led to substantially overestimated values in comparison with the experimental data. It is argued in Sen & Venkateswarlu (1983) and Zhou (1982) that this difference is due to three-dimensional effects which are not taken into account by the weakly nonlinear theories which they discuss (see also the discussion in Hocking *et al.* 1972) rather than due to the deficiency of the reduction schemes used to model the flow. On other hand, the disturbances introduced into the flow in the experiment by Nishioka *et al.* (1975) were generated by a ribbon vibrating across the complete channel width. This means that the initial excitation was essentially two-dimensional. Very small disturbance variations in the spanwise direction just repeated the form of imperfections of the primary flow which are attributed to minor warping of the top wall when machining access slits. Moreover, according to the scenario described in Nishioka & Asai (1984), the first step in transition is the amplification of a primary two-dimensional disturbance wave when the ribbon oscillation amplitude exceeds a certain threshold value. Only after this does the secondary bifurcation leading to three-dimensional distortions of the primary disturbance wave occur. This is also in accordance with the experiments by Karnitz, Potter & Smith (1974) who observed that in subcritical Poiseuille flow the sinusoidal disturbance wave with a frequency close to the one predicted by two-dimensional linear stability theory preceded a turbulent burst with an essentially flat front. Thus we believe that these experimental observations make the two-dimensional consideration of the initial stage of transition in plane Poiseuille flow and, in particular, determination of a threshold disturbance amplitude for two-dimensional disturbance waves reasonable.

In figure 9(*a*) we sketch the experimental threshold r.m.s. disturbance magnitude as a function of the non-dimensional excitation frequency $f(\alpha) = |\sigma^I(\alpha)|/(3Re)$ given by Nishioka *et al.* (1975) for Reynolds number 5000 if non-dimensionalization is made using the maximum flow speed and the channel half-width (corresponding to our Reynolds number which is larger by a factor 4/3). Symbols denote our predictions for threshold amplitudes $|A| = (-\sigma^R/K_1^R)^{1/2}$ obtained for plane disturbance waves at the corresponding frequencies. Note that according to Nishioka *et al.* (1975) the degree of basic flow three-dimensionality in their experiment was less than 6% in the worst case for Reynolds number 7500 which is beyond the linear stability boundary. For smaller Reynolds numbers the spanwise variation was substantially weaker. Thus comparison of their experimental results for the threshold amplitudes with our predictions based on a two-dimensional model is reasonable. Our results are in considerably better quantitative agreement with the experiment than those reported by Sen & Venkateswarlu (1983), and the form of the dependence of $|A(f)|$, for $0.26 \lesssim f \lesssim 0.34$, resembles the one given by Zhou (1982) in his figure 1(*a*) (two-dimensional disturbances as well were considered in both Sen & Venkateswarlu 1983 and Zhou 1982). On other hand, our results have some scatter. The scatter can be directly attributed to the influence of multiple resonances which exist between the mean flow correction and the $\alpha = 0$ harmonics (Suslov & Paolucci 1997) and which are not accounted for in the present analysis. The resonant frequencies are easily found at the intersections of lines $\sigma^R = -n^2\pi^2/2$, $n = 1, 2, \ldots$ with the $\sigma^R(f)$ curve for the leading eigenvalue shown in figure 9(*b*). The agreement between the present

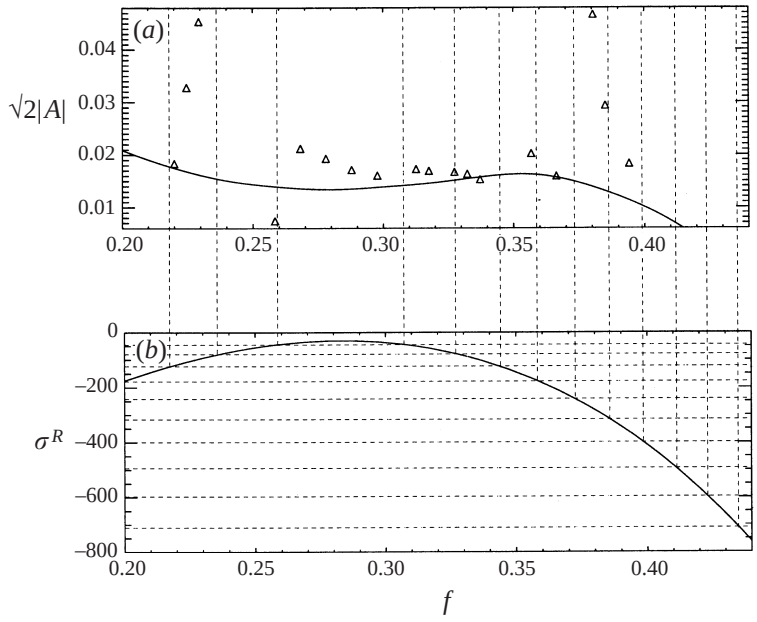

FIGURE 9. (*a*) Disturbance threshold amplitude curve from Nishioka *et al.* (1975); symbols denote values predicted by the present analysis. (*b*) Plane wave linear decay rate σ^R as a function of non-dimensional frequency for the Poiseuille flow at $Re = 4/3 \times 5000$; intersections of $\sigma^R = -n^2\pi^2/2$ $(n = 1, 2, \ldots)$ lines and the $\sigma^R(f)$ curve represent resonance points.

theoretical results and the experimental results in resonance-free frequency intervals is satisfactory, and thus we expect that our predictions for supercritical ($\sigma^R(\alpha) > 0$) flows, where no mean flow resonances exist, are sufficiently accurate.

Note also that the theory developed in Suslov & Paolucci (1997) enables one to model the evolution of a disturbance wave not necessarily corresponding to the wavenumber α (or frequency f) of the maximum linear amplification rate σ^R. In other words disturbance quantities can be computed and expansions can be made based on eigenfunctions of the linearized problem whose spatial period (and frequency of oscillation) differ from the critical ones. This enables us to consider a forced system where the frequency of the disturbances is prescribed by external means. Our calculations of K_1^R for Poiseuille flow at $Re = 4/3 \times 5000$ (not presented here) show that it becomes negative for $f \lesssim 0.22$ and $f \gtrsim 0.40$, which means that plane wave disturbances at these frequencies must decay no matter how big their initial amplitudes are. Thus, consistent with figure 10 in Sen & Venkateswarlu (1983), the predicted threshold amplitude increases rapidly outside the interval $0.22 \lesssim f \lesssim 0.40$, and no threshold amplitudes are computed for frequencies beyond this range as shown in figure 9*a*). The decrease in the experimental threshold amplitude outside this frequency range can be attributed to the development of localized rather than periodic disturbances. Turbulent spots in the laminar flow were observed in the experiment by Nishioka *et al.* (1975) in this frequency range, but they cannot be modelled within a discrete wave approach and require consideration of spatially modulated disturbance waves and wave packets.

5. Summary

We have developed a weakly nonlinear theory for the analysis of flows in open domains where the total mass of fluid might not be conserved. The theory is applied to the non-Boussinesq mixed convection flow of air in an open vertical channel with differentially heated walls. It is shown that constant mass flux and constant pressure gradient formulations result in distinct problems, which lead to qualitatively similar but quantitatively different results. The cubic Landau equation is shown to model the evolution of the disturbance amplitude for a wide range of governing parameters. Based on this equation the regions of supercritical and subcritical bifurcations are identified. Comparison of the present theory with those developed by Watson (1960) and Reynolds & Potter (1967) demonstrates the advantage of the current approach which is capable of providing better quantitative predictions for super- and subcritical flow regimes further from the marginally stable state.

Appendix

Functions entering the right-hand side of (45):

$$f_{20}^{(1)} = -\tfrac{8}{3}\mathrm{Re}\{\mathrm{D}(\mu_{11}\,\mathrm{D}u_{11}^*)\} + 2\alpha\,\mathrm{Im}\{\tfrac{2}{3}\,\mathrm{D}(\mu_{11}v_{11}^*) - \rho_{00}u_{11}v_{11}^* + \rho_{11}u_{11}^*v_{00}\}$$
$$+ \rho_{00}\,\mathrm{D}|u_{11}|^2 + 2\mathrm{Re}\{\sigma\rho_{11}^*u_{11}\},$$

$$f_{20}^{(2)} = 2\mathrm{Re}\{\rho_{00}u_{11}\,\mathrm{D}v_{11}^* + \rho_{11}u_{11}^*\,\mathrm{D}v_{00} - \mathrm{D}(\mu_{11}\,\mathrm{D}v_{11}^*)\} + 2\alpha\,\mathrm{Im}\{\rho_{11}v_{11}^*v_{00} - \mathrm{D}(\mu_{11}v_{11}^*)\}$$
$$+ \overline{\Pi}_{20} - \mathrm{D}(\mu_{00TT}|T_{11}|^2\,\mathrm{D}v_{00}) + \frac{Gr}{2\epsilon}\rho_{00TT}|T_{11}|^2 + 2\mathrm{Re}\{\sigma\rho_{11}^*v_{11}\},$$

$$f_{20}^{(3)} = 2\mathrm{Re}\left\{c_{p00}(\rho_{00}\,\mathrm{D}T_{11}u_{11}^* + \rho_{11}\,\mathrm{D}T_{00}u_{11}^*) + c_{p11}\rho_{00}\,\mathrm{D}T_{00}u_{11}^* - \frac{1}{Pr}\,\mathrm{D}(k_{11}\mathrm{D}T_{11}^*)\right\}$$
$$+ 2\alpha c_{p00}\mathrm{Im}\{c_{p00}(\rho_{11}T_{11}^*v_{00} - \rho_{00}T_{11}v_{11}^*) + c_{p11}\rho_{00}T_{11}^*v_{00}\}$$
$$- \frac{1}{Pr}\mathrm{D}(k_{00TT}|T_{11}|^2\,\mathrm{D}T_{00}) + 2\mathrm{Re}\{\sigma(c_{p00}\rho_{11}^* + c_{p11}^*\rho_{00})T_{11}\},$$

$$f_{20}^{(4)} = -2\mathrm{Re}\{\mathrm{D}(\rho_{11}u_{11}^*)\} + 2\sigma^R\rho_{00TT}|T_{11}|^2,$$

where for the variable properties used

$$c_{p11} = c_{p20} = c_{p22} = 0, \quad \rho_{00TT} \equiv \frac{\partial^2\rho_{00}}{\partial T_{00}^2} = 2\frac{\rho_{00}}{T_{00}^2},$$

$$\mu_{00TT} \equiv \frac{\partial^2\mu_{00}}{\partial T_{00}^2} = -\frac{1+S_\mu}{4}\frac{T_{00}^2 + 6S_\mu T_{00} - 3S_\mu^2}{\sqrt{T_{00}}(T_{00}+S_\mu)^3},$$

$$k_{00TT} \equiv \frac{\partial^2 k_{00}}{\partial T_{00}^2} = -\frac{1+S_k}{4}\frac{T_{00}^2 + 6S_k T_{00} - 3S_k^2}{\sqrt{T_{00}}(T_{00}+S_k)^3}.$$

REFERENCES

Chenoweth, D. R. & Paolucci, S. 1985 Gas flow in vertical slots with large horizontal temperature differences. *Phys. Fluids* **28**, 2365–2374.

Chenoweth, D. R. & Paolucci, S. 1986 Natural convection in an enclosed vertical air layer with large horizontal temperature differences. *J. Fluid Mech.* **169**, 173–210.

Davey, A., Hocking, L. & Stewartson, K. 1974 On the nonlinear evolution of three-dimensional disturbances in plane Poiseuille flow. *J. Fluid Mech.* **63**, 529–536.

Davey, A. & Nguyen, H. P. F. 1971 Finite-amplitude stability of pipe flow. *J. Fluid Mech.* **45**, 701–720.

Fröhlich, J., Laure, P. & Peyret, R. 1992 Large departures from Boussinesq approximation in the Rayleigh–Benard problem. *Phys. Fluids* **4**, 1355–1371.

Fujimura, K. 1989 The equivalence between two perturbation methods in weakly nonlinear stability theory for parallel shear flows. *Proc. R. Soc. Lond.* A **424**, 373–392.

Fujimura, K. & Mizushima, J. 1987 Nonlinear interaction of disturbances in free convection between vertical parallel plates. In *Nonlinear Wave Interactions in Fluids* (ed. R. W. Miksad, T. R. Akylyas & T. Herbert), pp. 123–130.

Glendinning, P. 1984 *Stability, Instability and Chaos: an Introduction to the Theory of Nonlinear Differential Equations*, pp. 78–83. Cambridge University Press.

Herbert, T. 1983 On perturbation methods in nonlinear stability theory. *J. Fluid Mech.* **126**, 167–186.

Hocking, L., Stewartson, K., Stuart, J. T. & Brown, S. N. 1972 A nonlinear instability burst in plane parallel flow. *J. Fluid Mech.* **51**, 705–735.

IMSL, Inc. 1989 *IMSL Mathematical Library, Version 1.1*. Houston, TX.

Karnitz, M., Potter, M. & Smith, M. 1974 An experimental investigation of transition of a plane Poiseuille flow. *Trans. ASME* I: *J. Fluids Engng* **96**, 384–388.

Mizushima, J. & Gotoh, K. 1983 Nonlinear evolution of the disturbance in a natural convection induced in a vertical fluid layer. *J. Phys. Soc. Japan* **52**, 1206–1214.

Nishioka, M. & Asai, M. 1984 Evolution of Tollmien–Schlichting waves. In *Turbulence and Chaotic Phenomena in Fluids* (ed. T. Tatsumi), pp. 87–92. Elsevier.

Nishioka, M., Iida, S. & Ichikawa, Y. 1975 An experimental investigation of the stability of plane Poiseuille flow. *J. Fluid Mech.* **72**, 731–751.

Paolucci, S. 1982 On the filtering of sound from the Navier–Stokes equations. *Tech. Rep.* SAND82-8257. Sandia National Laboratories, Livermore, California.

Reynolds, W. C. & Potter, M. C. 1967 Finite-amplitude instability of parallel shear flows. *J. Fluid Mech.* **27**, 465–492.

Sen, P. K. & Venkateswarlu, D. 1983 On the stability of plane Poiseuille flow to finite-amplitude disturbances, considering higher-order Landau coefficients. *J. Fluid Mech.* **133**, 179–206.

Stewartson, K. & Stuart, J. T. 1971 A non-linear instability theory for a wave system in plane Poiseuille flow. *J. Fluid Mech.* **48**, 529–545.

Stuart, J. T. 1960 On the non linear mechanics of wave disturbances in stable and unstable parallel flows. Part 1. The basic behaviour in plane Poiseuille flow. *J. Fluid Mech.* **9**, 353–370.

Suslov, S. A. 1997 Nonlinear analysis of non-Boussinesq convection. PhD thesis, University of Notre Dame, USA.

Suslov, S. A. & Paolucci, S. 1995*a* Stability of natural convection flow in a tall vertical enclosure under non-Boussinesq conditions. *Intl J. Heat Mass Transfer* **38**, 2143–2157.

Suslov, S. A. & Paolucci, S. 1995*b* Stability of mixed-convection flow in a tall vertical channel under non-Boussinesq conditions. *J. Fluid Mech.* **302**, 91–115.

Suslov, S. A. & Paolucci, S. 1997 Nonlinear analysis of convection flow in a tall vertical enclosure under non-Boussinesq conditions. *J. Fluid Mech.* **344**, 1–41.

Suslov, S. A. & Paolucci, S. 1999 Nonlinear stability of mixed convection flow under non-Boussinesq conditions. Part 2. Mean flow characteristics. *J. Fluid Mech.* **398**, 87–108.

Watson, J. 1960 On the non-linear mechanics of wave disturbances in stable and unstable parallel flows. Part 2. The development of a solution for plane Poiseuille flow and for plane Couette flow. *J. Fluid Mech.* **9**, 371–389.

White, F. M. 1974 *Viscous Fluid Flow*. McGraw-Hill.

Yao, L. S. & Rogers, B. B. 1992 Finite-amplitude instability of non-isothermal flow in vertical annulus. *Proc. R. Soc. Lond.* A **437**, 267–290.

Zhou, H. 1982 On the non linear theory of stability of plane Poiseuille flow in the subcritical range. *Proc. R. Soc. Lond.* A **381**, 407–418.